American Superconductor™

REVOLUTIONIZING THE WAY THE WORLD USES ELECTRICITY™

Contract No. DE-FG02-07ER86300

Department of Energy

Low AC Loss YBCO Coated Conductor Geometry by Direct Inkjet Printing

Final Report

October 2009

Prepared by:
Dr. Martin Rupich
American Superconductor Corporation
Devens, Massachusetts, 01434

and

Dr. Robert Duckworth
Oak Ridge National Laboratory
Oak Ridge, Tennessee 37831

Approved for Public Release

Table of Contents

EXECUTIVE SUMMARY

The second generation (2G) high temperature superconductors (HTS) wire offers potential benefits for many electric power applications, including ones requiring filamentized conductors with low ac loss, such as transformers and fault current limiters. However, the use of 2G wire in these applications requires the development of both novel multi-filamentary conductor designs with lower ac losses and the development of advanced manufacturing technologies that enable the low-cost manufacturing of these filamentized architectures. This Phase I SBIR project focused on testing inkjet printing as a potential low-cost, roll-to-roll manufacturing technique to fabricate potential low ac loss filamentized architectures directly on the 2G template strips.

PROJECT OBJECTIVES

The primary objective of this DOE SBIR/STTR project was the evaluation of the technical and practical feasibility of direct inkjet printing of a patterned YBCO films as a low cost, scaleable method for manufacturing low ac loss 2G HTS wire.

The Phase I project focused specifically on:

- Direct inkjet printing and processing of filamentized YBCO conductors on RABiTS templates in lengths to 10 cm using a bench-top inkjet printing station.
- Characterization of the inkjet-printed YBCO films
- Measurement of ac loss in selected filamentized YBCO architectures on YBCO(MOD)/RABiTS based conductors.
- Assessment of inkjet as a practical roll-to-roll manufacturing technique

TECHNICAL APPROACH

The availability of second generation (2G) superconducting YBCO wire offers the opportunity to develop HTS motors, transformers, inductors or generators; enabling the development of lightweight, compact, high-power devices for a numerous commercial and military uses. AMSC has established an initial manufacturing line that produces 2G wire in lengths of 400 meter with critical currents approaching 250 A/cm-w (77K, self-field) [1, 2, 3, 4, 5, 6, 7]. AMSC's manufacturing process is based on combining low-cost metal organic deposition (MOD) of the YBCO layer with a RABiTS^{TM}-type template [8,9,10,11,12] as illustrated in Figure 1. The typical wire produced consists of a continuous YBCO film with a width of 4 mm and thickness of ~0.8 μm as show in the transverse cross-section image in Figure 2.

Although the 2G wire, now being manufactured, is suitable for many types of electric power devices, including motors and power transmission cables, the ac losses from the wide YBCO conducting layers are too high for use in the synchronous generator armature windings and compact transformers of interest for military applications. It has been demonstrated that the ac loss of $YBa_2Cu_3O_7$ (YBCO) coated conductor can be minimized by dividing the YBCO film into thin filament arrays such as illustrated in Figure 3 [13,14,15,16]. However, this approach lowers the effective current density of the whole wire due to the concomitant reduction of the HTS material within the wire package. Therefore, the structure of the electrical wire must be optimized and the striated filaments must maintain the Jc of the un-patterned films to obtain large critical currents with minimized ac loss necessary for the targeted applications.

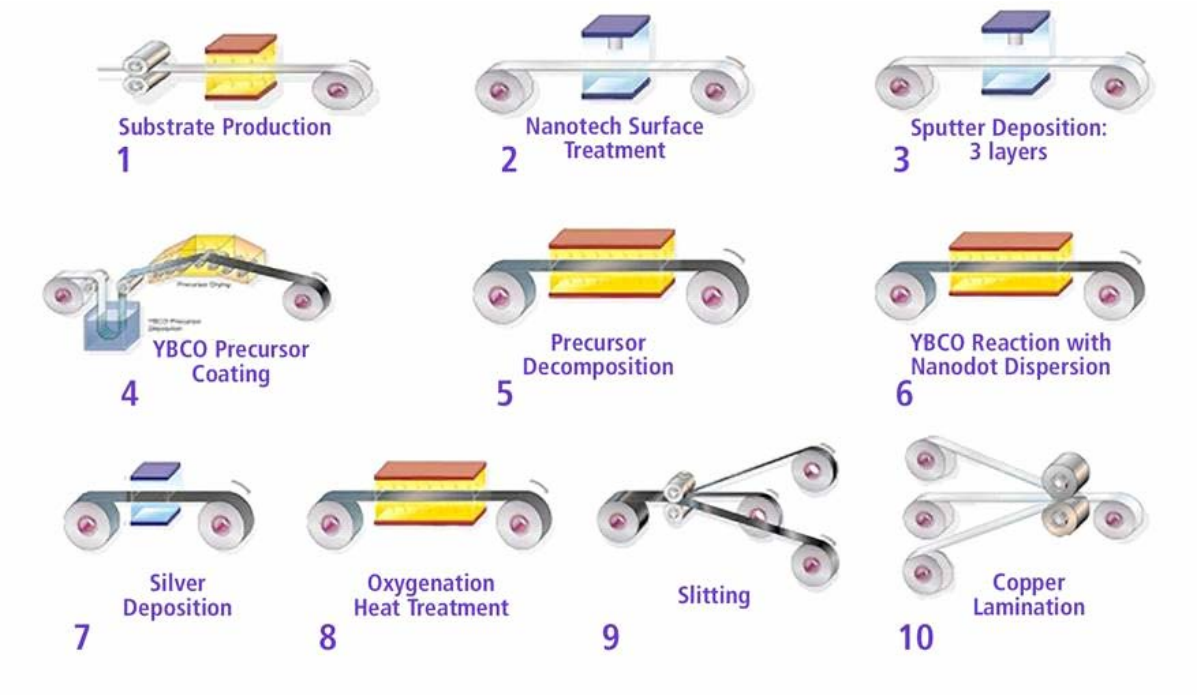

Fig. 1. Illustration of the steps in AMSC's 2G manufacturing process. The proposed inkjet printing would replace the current slot die coating and Ag deposition.

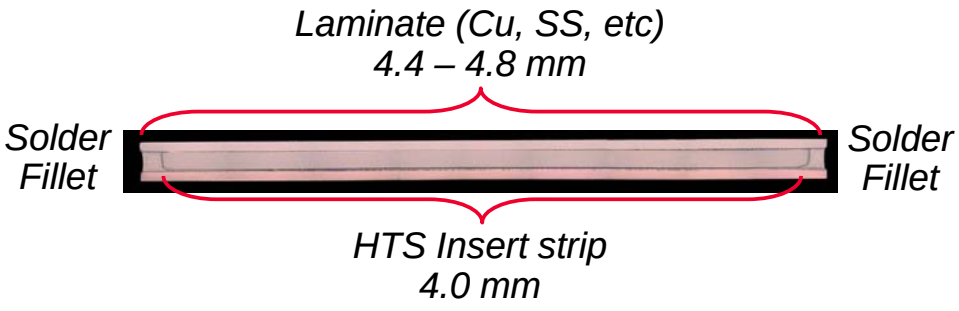

Fig. 2. Transverse cross-section of ASMC's 344 superconductor wire.

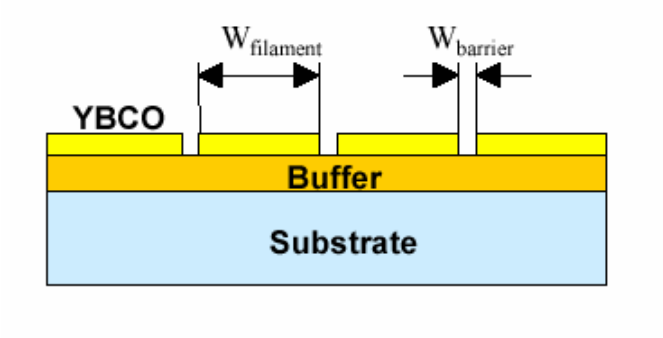

Fig. 3. Targeted architecture of a striated, multifilamentary YBCO film.

Numerous options have been proposed for produce the necessary striated YBCO film architecture shown in Figure 3; however, no standard method has been demonstrated that is applicable to *low-cost* manufacturing of practical conductors. A major requirement of the processing is the need to form the superconducting layer precisely, with gaps ideally less than fifty microns wide, to insure the filaments are not bridged, and to insure that the patterned filaments individually have a Jc comparable to the un-patterned film. The general approaches previously used for this work have been laser ablation or photolithography/chemical etching; however, such processing is expensive, and there are attendant concerns that re-deposition of the removed YBCO and thermal or chemical damage to the residual filaments can cause degradation of the critical temperature and critical current density of the film. In addition, both of these processes remove a significant fraction of the YBCO layer, adding to the cost of the overall conductor.

In contrast, inkjet printing is a direct write drop-on-demand (DOD) process widely used for printing in a wide range of commercial and industrial applications. Although the technique is widely used for printing text and graphics, it has many advantages for direct printing of materials deposition. In principal, inkjet printing is equivalent to the slot die coating technique used in ASMC's roll-to-roll manufacturing line. In both techniques, an ink containing the constituents of the YBCO superconductor is deposited on the RABiTS template. In the case of the slot die process, the ink is deposited as a continuous sheet uniformly across the entire surface of the template; while with the inkjet technique, the ink is deposited drop-by-drop in discrete locations on the template. When the drops are positioned to overlap, resulting in complete coverage of the template, the two techniques are virtually indistinguishable. In fact the inkjet process has been used to print continuous YBCO films [17,18]. The major advantage if inkjet printing is the ability to print the YBCO in discrete patterns such as the striated filaments architectures identified as useful for low ac loss wires.

The focus of this program was to evaluate the structure, critical current and ac loss characteristics of filamentized YBCO conductors fabricated by direct inkjet-printing on commercial RABiTS templates and assess its use as a practical, low-cost mroll-to-roll manufacturing technique.

PHASE I RESULTS

Task 1: Inkjet Printing of YBCO Filaments

The primary focus of this task was to optimize deposition and processing of suitable YBCO precursor inks using a bench top house inkjet printing facility for characterization with respect to critical current and ac loss. The effort was carried out at ORNL and AMSC.

RABiTS templates were produced by AMSC using its 2G production line at its manufacturing facility in Devens, Massachusetts. The basic structure of the RABiTS template consists of a Ni5%W substrate with epitaxial layers of Y_2O_3, YSZ and CeO_2 as show schematically in Fig. 4. Samples used for this project were cut from continuous lengths (~100m) of 40mm wide templates strips.

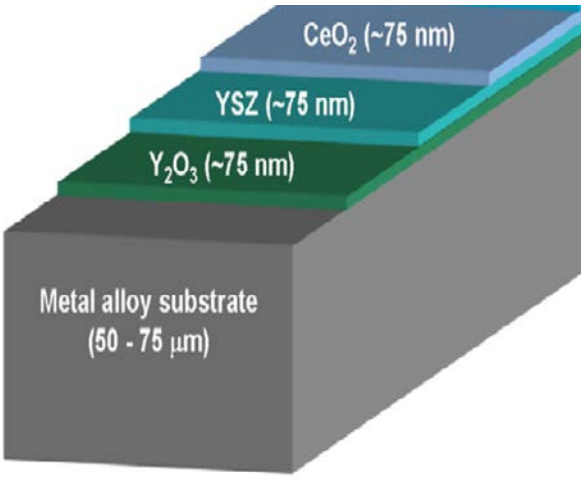

Fig. 4. Schematic illustration of the RABITS template with the architecture: CeO_2/YSZ/Y_2O_3/Ni5%W). The buffer layers are deposited by reactive sputtering.

The YBCO precursor ink was prepared from AMSC's standard YBCO precursor solution. The solution concentration and viscosity was modified by addition of organic and/or aqueous additives to optimize solution viscosity and partial pressure for the specific piezoelectric print heads.

Inkjet printing of the YBCO films was carried using a MicroFab Technologies, Inc. printing station available at ORNL. The printing station, shown in Figure 5, employs a single-nozzle piezoelectric print head coupled with a computer-controlled, precision x-y stage. The ink reservoir and dispenser were in a fixed location and the RABiTS substrate was attached to the translation table. Filament patterns were generated with standard drafting software and are converted to motion control commands sent to the translation table. The filamentary patterns were printed by synchronizing inkjet droplet delivery with the table motion. The ink was dispensed in ~ 50μm droplets. The droplet formation was continuously monitored by a high speed camera.

Thermal processing of the printed films was carried out in static, short sample laboratory furnaces available at both AMSC and ORNL.

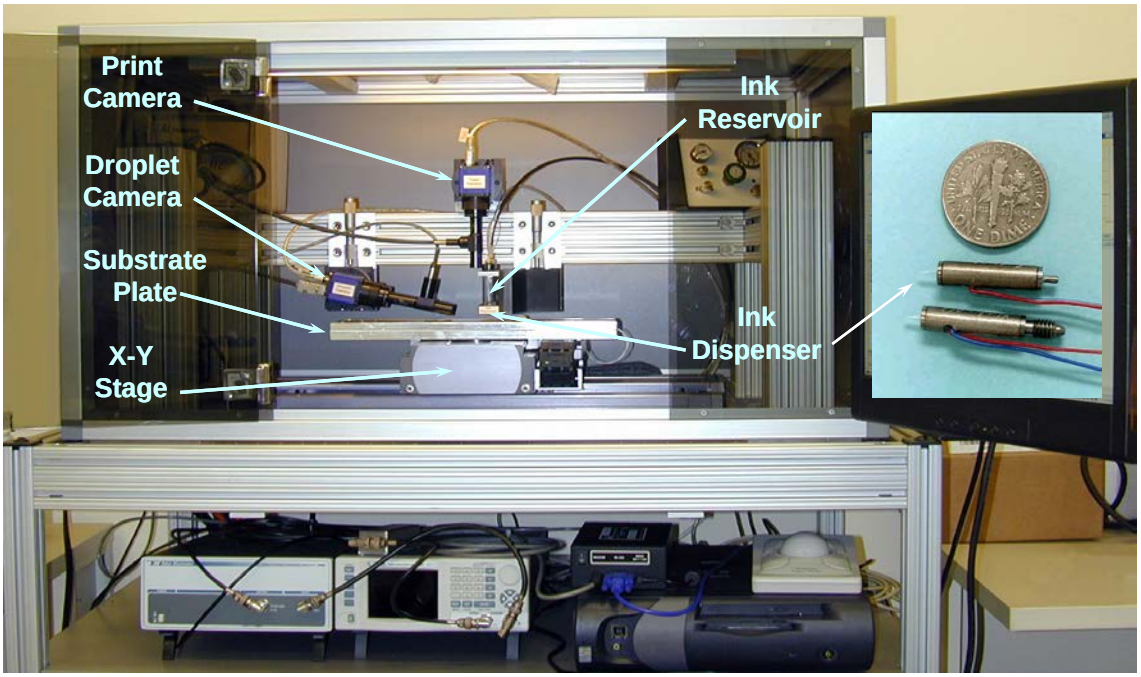

Fig. 5. Inkjet printing station used during the Phase I project. Relative size of inkjet print heads is shown in the inset at the right.

Various printing conditions, precursor ink formulations and processing protocols were evaluated for the printing of the YBCO with various filament widths and spacing. The structure and shape of the YBCO filaments were evaluated after inkjet printing, after the pyrolysis (burnout of organics) and conversion to the YBCO phase. As seen in the diagram in Figure 6, throughout the processing steps, the filaments contract in the thickness direction only, with virtually no change in the lateral dimensions. Unlike filaments prepared by removal processes (i.e. etching or laser ablation) the inkjet-printed filaments have rounded edges rather than square edges. This reflects the wetting of the substrate by the ink and the surface tension. This effect is minimized as the filament width increases.

Cracking can occur during large volume change associated with the pyrolysis process as seen in Figure 6. This is similar to the thickness changes occurring in the continuous films deposited by slot die coating. Filament cracking was minimized by optimizing the ink compositions and pyrolysis process using a small laboratory furnace fitted with an optical window as seen in Figure 7.

Figure 8 shows the cross-sections thickness profile of a series of 1 mm wide filaments after the pyrolysis step as a function of thickness. For samples with a thickness less than 2.5 μm (equivalent to ~1.1 μm YBCO), the decomposed filaments were smooth, crack-free, and uniform along the length. However, for thicker filaments, cracking occurred during the pyrolysis process. This is reflected in the high frequency roughness in the profilimitey measurements in Figure 8.

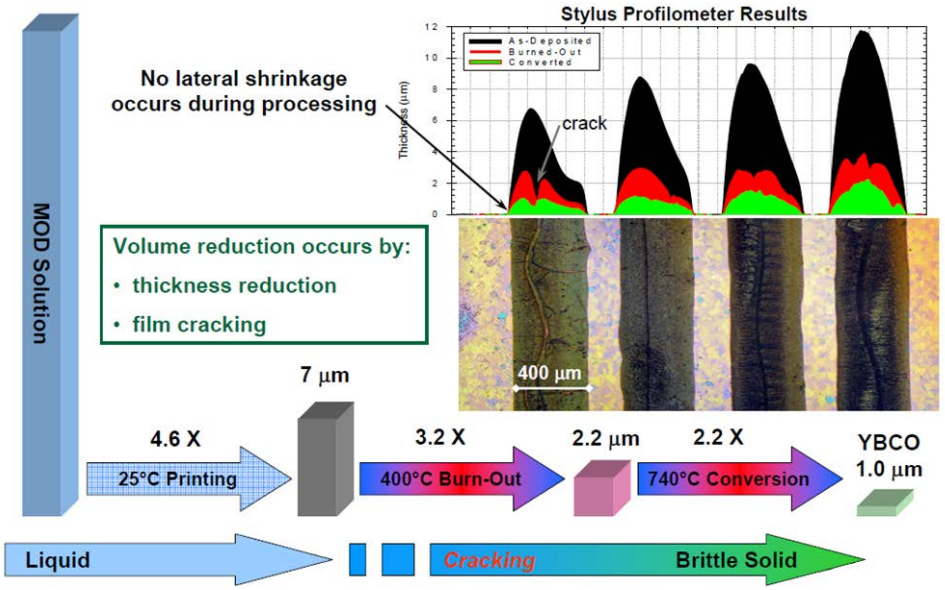

Fig. 6. Through thick shrinkage occurs during the printing, pyrolysis and conversion stages. No lateral shrinkage or spreading occurs during any os the steps. Cracking occurs during the pyrolysis step and can be controlled by the process parameters. (Note the ~60X difference in the thickness and width scales.)

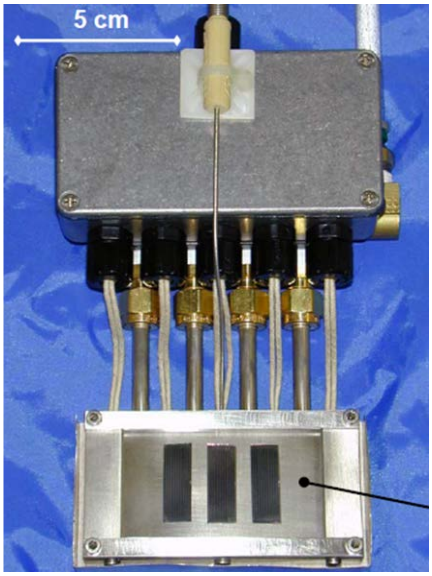

Fig. 7. Laboratory furnace with optical window used to optimize pyrolysis of inkjet-printed YBCO filaments.

The thickness profiles after pyrolysis of constant thickness (~2.2 μm) filaments are shown in Figure 9 as a function of filament width. The decrease in thickness observed with the narrower filaments is a consequence of spreading of the ink that occurs at the edges of each filament.

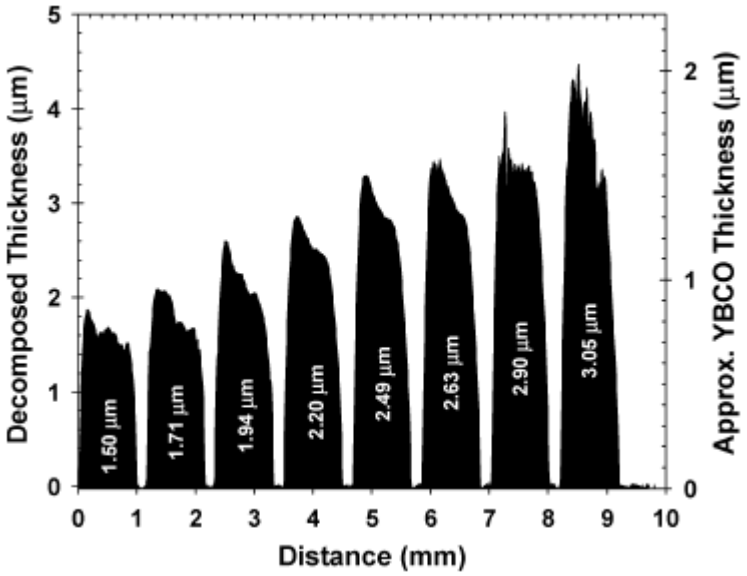

Fig. 8. Cross-sectional filament profiles after decomposition as a function of filament thickness. The average decomposed precursor filament thickness is indicated for each filament. The roughness for the thickest three filaments is associated with microscopic cracking during the pyrolysis step.

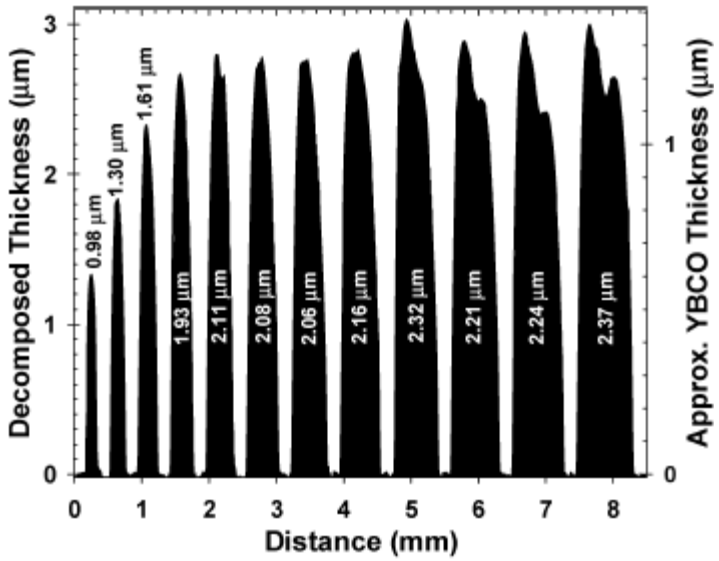

Fig. 9. Cross-sectional filament profiles, after pyrolysis, as a function of filament width. The average thickness is indicated for each filament.

The conversion process was also examined as a function of filament width by monitoring the YBCO formation using an in-situ x-ray system. Five filamentary precursor samples were

studied. Each sample consisted of an array of parallel filaments of equal width, thickness and gap spacing between filaments. The target YBCO thickness for all filaments was 1 μm and the filament spacing 100 μm. The filament widths ranged from 0.25 to 4.0 mm. All filaments were processed with the same conditions previously established for comparable thickness continuous films.

X-ray diffraction analysis of processed filaments, shown in Figure 10, shows the conversion rate increased with decreasing filament width, with the average rate increasing from 3.0 Å/s for 4-mm wide filaments to 4.8 Å/s for 250-μm wide filaments. This is the result of two factors. The first is the change in the ambient $[HF]_g$ that depends on the ratio of the filament width and filament-to-filament spacing of the sample. The second factor is the non-uniform cross-section thickness of the inkjet-printed filaments that results from the ink viscosity and ink/substrate interface. As the filament width decreases, the edge zones account for a larger percentage of the individual filament width, thus reducing the effective filament thickness.

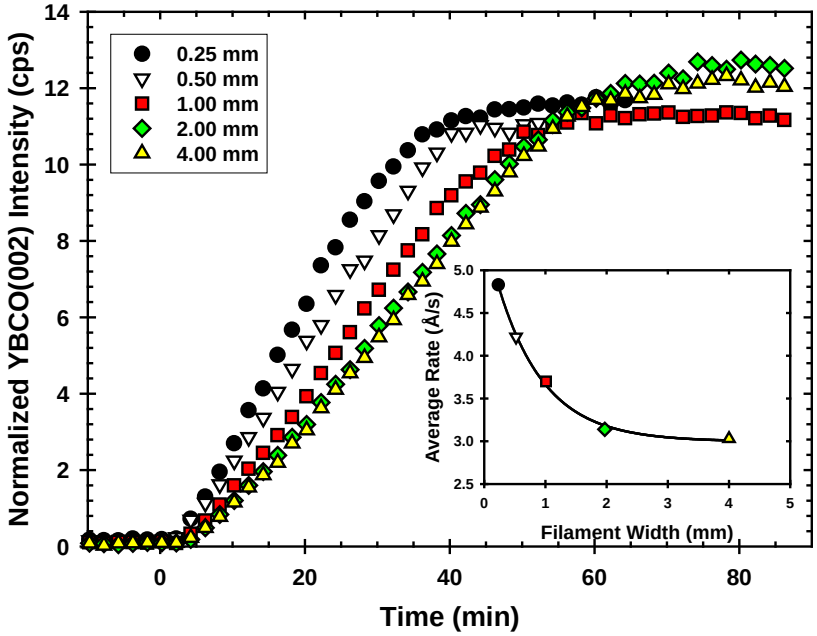

Fig. 10. X-ray diffraction spectrum (normalized intensity of the YBCO(002) peak) as a function of processing time for inkjet-printed YBCO films with different filament widths.

The critical current of each sample was measured at 77K, self-field using a standard transport technique. The normalized critical current (A/cm-w) dropped with decreasing filament width as shown in Figure 11. To confirm that the decrease in critical current was associated with the processing of the narrower filaments and not simply the result of a percolative current path on the RABiTS templates, a standard YBCO film, prepared at AMSC, was laser patterned to various widths. The I_c (total contribution for all the parallel filaments (i.e., 1 each of 4 mm width, 2 each for 2 mm width, …, 64 each for 63 μm width) was measured after each sequential scribing of the sample to narrower filament widths. As seen in Figure 12, the laser patterned sample showed behavior consistent with percolation-limited current flow, confirming that the

lower currents obtained with the inkjet-printed filaments is the result of filament structure and growth issues.

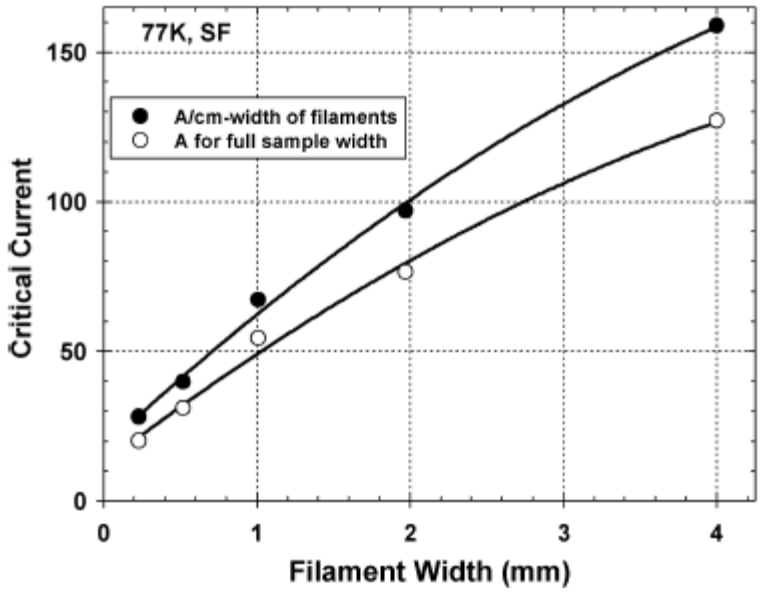

Fig. 11. Comparison of the measured critical current, normalized to A/cm-width, (77K, sf) as a function of filament width (●). Critical current is also plotted for the full sample width (○).

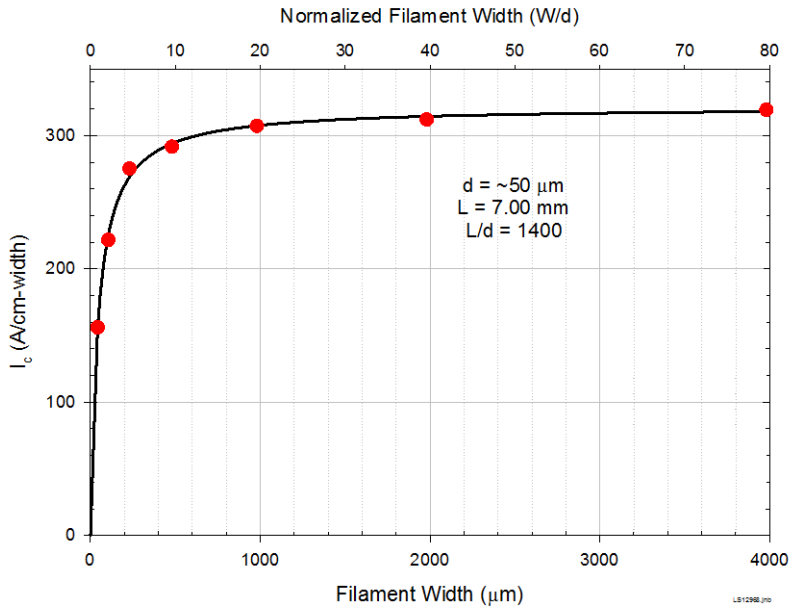

Fig. 12. A laser-scribed AMSC YBCO filamentary conductor shows behavior consistent with percolation-limited current flow. The Ic limiting defect size (grain size) is assumed to be ~50 μm).

It is believed that the lower critical currents are the result of the non-uniform filament cross-sections and the presence of multiple filament edges as shown in Figure 13. Studies of the BaF_2 based MOD process have shown that the ideal growth conditions depend on the film thickness and that the growth rate differs at the center and edges of the film. These results suggest that it will be difficult to achieve critical currents in the filamentized, inkjet-printed YBCO films comparable to that achieved in the un-patterned YBCO films.

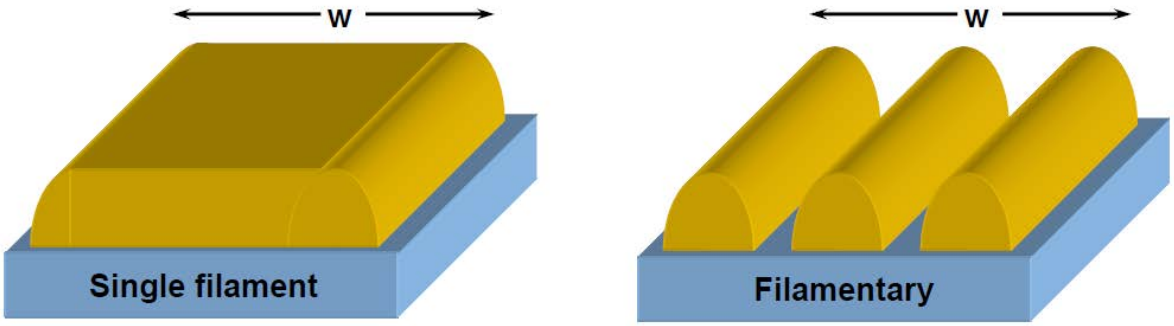

Fig. 13. Schematic illustration showing the differences in the precursor thickness and the number of film edges for an un-patterned YBCO film and an filamentized YBCO film deposited by inkjet printing. The ideal growth YBCO conditions are affected by both the average film thickness and the number of film edges present.

Task 2: Benchmarking ac Loss in Micro-bridged YBCO Filament Architecture

Samples with individual filament length approaching 10-cm were printed on the RABiTS templates using the optimized processing parameters and conversion to YBCO using the standard processing conditions. The inkjet-printed films had well-defined YBCO filaments separated by discrete gaps. Figures 14 and 15 show examples of inkjet-printed films printed in arrays of 11 and 30 individual YBCO filaments with filament spacing on the order of 100 μm. In 1-cm wide tapes, with the same critical current density, gaps of this size are calculated to reduce the current carrying capacity by a factor 10% for 11-filament conductors and 40% for the 30-filament conductors.

Characterization of ac loss was also carried out on the inkjet-printed filaments. AC loss was measured calorimetrically as a function of field and frequency at 77 K [19]. Figure 16 shows the ac loss at 60 Hz as a function of the peak perpendicular field for the inkjet-printed filamentary YBCO coated conductor with the pattern shown in Figure 14 (11 filaments, 800 μm width and 100 μm spacing) with a critical current of 61 A. The ac loss for an un-patterned YBCO coated conductor, with a critical current of 190 A, is shown for comparison. In order to compare the ac loss between the two samples, the Brandt model [20] was used to calculate the hysteretic loss and plotted in Figure 16. It is clear from the plots that the inkjet filamentary conductor exhibited higher than predicted ac loss compared to the model calculations. When the frequency was

taken into account and the rationalized ac loss plotted with respect to the product of the peak perpendicular field and the frequency, it was obvious that some coupling mechanism was present in the films as seen in Figure 17. The presence of coupling loss was also observed in other inkjet-printed filamentary YBCO coated conductors that were fabricated with ORNL precursor inks and different processing conditions on AMSC templates [19]. It was speculated that the coupling was related to the filament structure, thus additional experiments were carried out to study potential mechanisms.

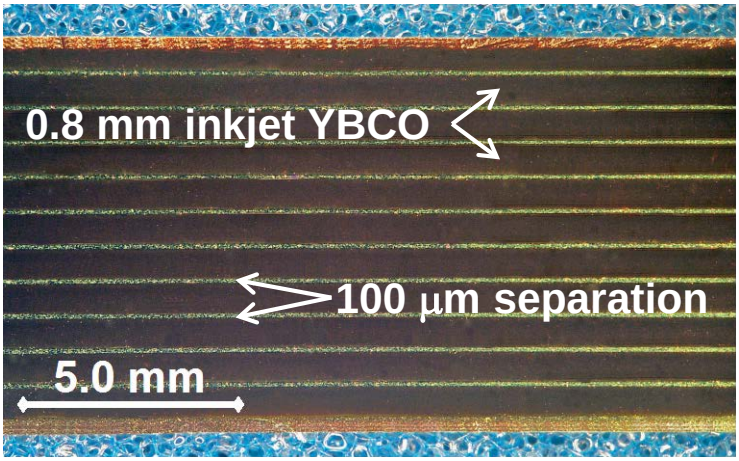

Fig. 14. Optical micrograph of an 11 filament, inkjet-printed YBCO conductor with an average filament width of 800 μm and average spacing of 100 μm between the filaments.

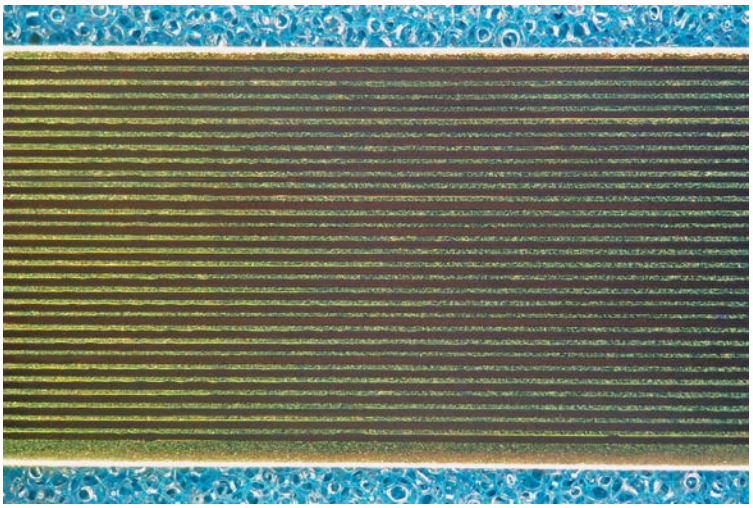

Fig 15. Optical micrograph of a 30 filament, inkjet-printed YBCO conductor with an average filament width of 200 μm and average spacing of 100 μm between the filaments.

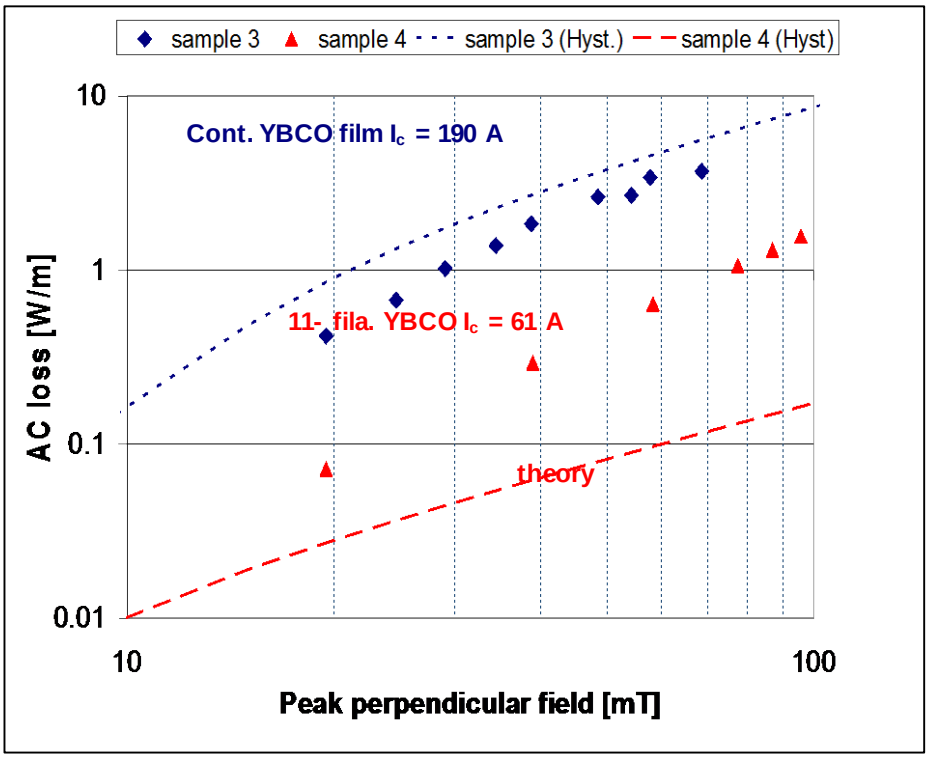

Fig 16. AC loss as a function of peak perpendicular field at 60 Hz and 77 K for a 11-filament inkjet-based YBCO coated conductor with a critical current at 77 K of 61 A and for a continuous YBCO coated conductor with a critical current of 190 A. The dashed lines show the theoretical ac loss for each sample predicted by the Brandt model.

In an effort to elucidate the root cause mechanism for the coupling observed in the inkjet-printed YBCO filamentary conductors, further investigation was done to study the structure of the YBCO filaments after deposition. Optical imaging of the filaments showed undulations along the edges of some of the converted filaments as shown in Figure 18. These undulations were present with all the ink formulations tested for the YBCO printing. It is believed the undulations are associated with the speed the printed head moves across the tape length/width and the resultant interaction of neighboring droplets. However, this mechanism was not conclusively confirmed during the Phase I project.

To determine whether this undulation was a factor in higher than expected ac loss, a series of samples were fabricated with un-patterned YBCO coated conductors from AMSC. After the silver cap layer was removed via chemical etching, laser scribing was utilized to produce an undulated filament structure where a triangular shaped undulation with a width of 200 μm and a spacing of one undulation every 1-mm as shown in Figure 19. A comparison sample with straight 1-mm wide filaments was also produced via laser scribing and both samples were annealed in an oxygen atmosphere to remove coupling associated with the damage produced via laser scribing.

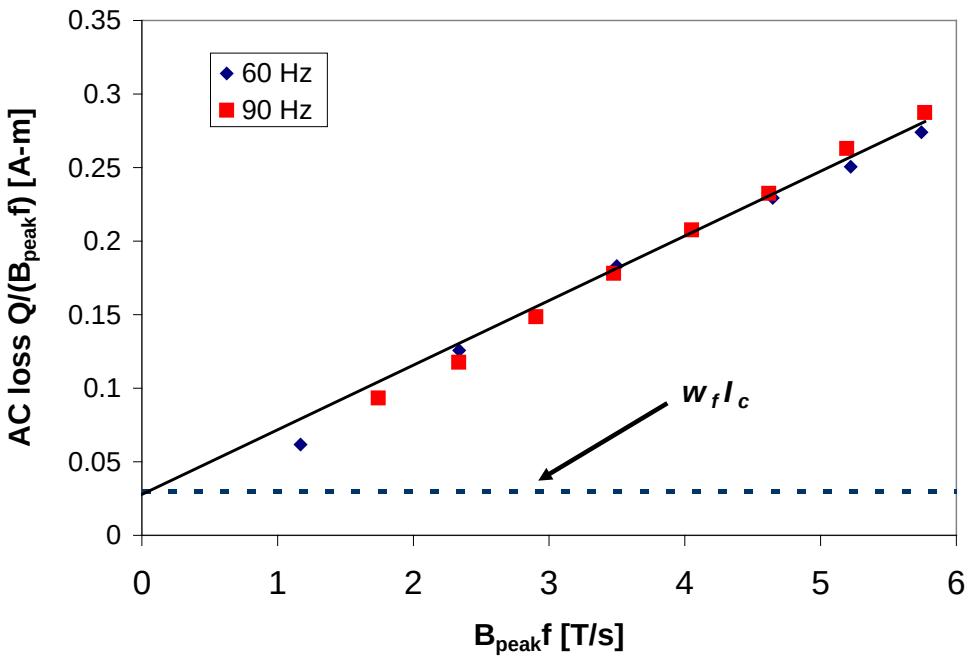

Fig. 17. Frequency dependence of rationalized ac loss at 77 K with respect to product of peak perpendicular field and frequency for 11-filament inkjet-based YBCO coated conductor with critical current at 77 K of 61 A.

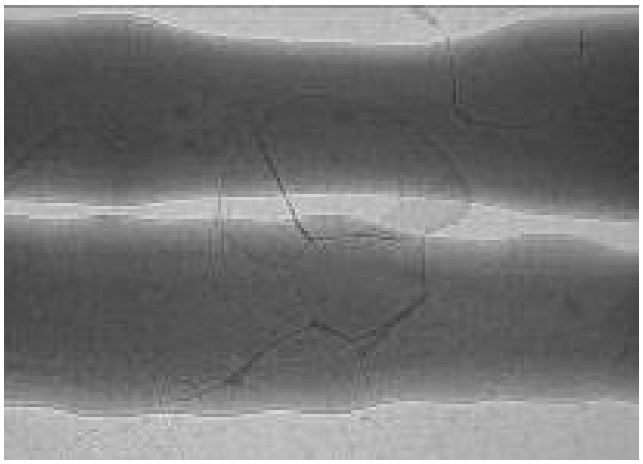

Fig. 18. Optical image of undulations observed in inkjet-deposited YBCO filaments.

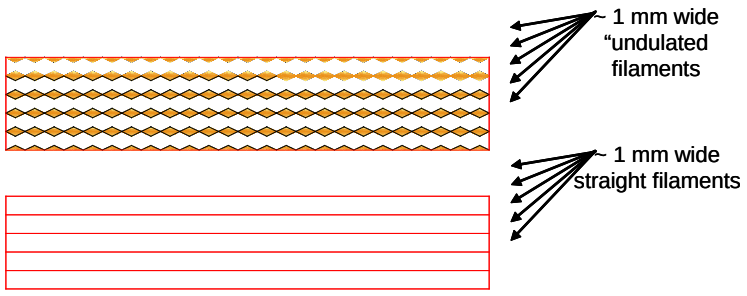

Fig. 19. Geometry of YBCO filaments with "undulated" structure introduced via laser scribing.

AC loss was measured at 77 K as a function of peak perpendicular field and frequency for the both the undulated and straight filament patterns shown in Figure 19. The samples had an average filament width of 1 mm and an average filament gap of 50 μm. As seen in Figure 20, the ac loss in the undulated structure, at 60 Hz, was measurably higher than the ac loss in straight filament structure. However, when the frequency dependence of the ac loss for the undulated structure was taken into account, the losses were considered hysteretic in nature and not coupling since there was not a linear dependence on the rationalized ac loss as shown in Figure 21.

Although the undulated structure appeared to impact the superconducting hysteretic loss in these samples, it was not the source of the observed coupling seen previously. No other root cause of the apparent coupling was identified during the project.

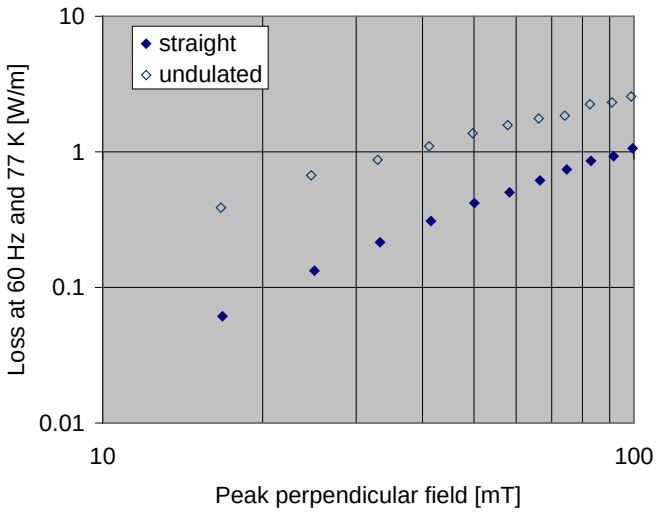

Fig. 20. AC loss as a function of peak perpendicular field at 60 Hz and 77 K for two 10-filament YBCO coated conductors with either straight or undulated filaments along the length as shown in Figure 18.

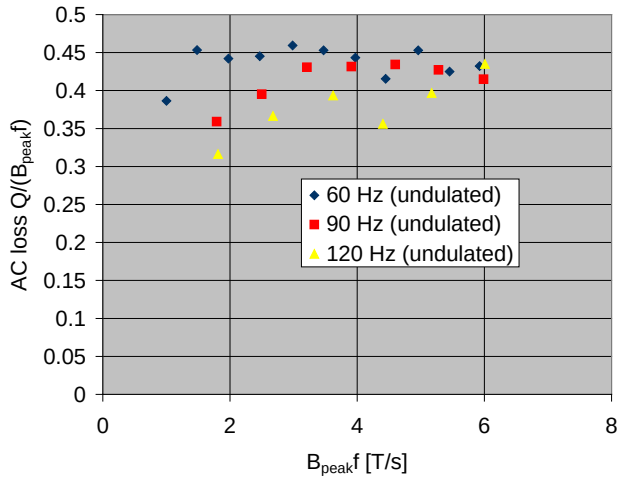

Fig. 21. Frequency dependence of rationalized ac loss at 77 K with respect to product of peak perpendicular field and frequency for 10-filament YBCO coated conductors with undulated filaments along the length as shown in Figure 18.

Task 3. Direct Inkjet Printing of Low ac Loss Conductors Architectures

The low critical current and poor ac-loss reduction achieved of the samples produced and characterized in Tasks 1 and 2 suggest that direct inkjet-printing of YBCO is not currently a viable low-cost manufacturing process for fabricating finely patterned YBCO films for potential low-ac loss architectures. The major issues are the reduced normalized critical current of the inkjet-printed samples and the unidentified coupling losses. Since the simple striated filament patterns did not achieve the meet the minimum requirements (minimum Jc loss and coupling), the printing of more complex patterns was not pursued in the Phase I program.

However, the inkjet print technique was also tested as a means to deposit a resist on the un-patterned YBCO films. In these experiments, inkjet printing was used print resist materials directly on to YBCO coated conductors and then the un-coated regions were removed by chemical etching leaving behind a filamentary structure. The process is illustrated in Figure 22, where starting with silver-stabilized YBCO coated conductor, a chemical resist is deposited along the conductor in well-defined regions. After the chemical resist cures, a hydrogen peroxide/ammonia solution was used to chemically etch the silver and a diluted phosphoric acid solution was used to remove the YBCO in those areas not covered by the chemical resist. The method should produce filaments with the printed structure and provide a means to change the filament pattern along length when the resist is printed in a larger scale system.

Development of the inkjet printing was initially tested in-house. However, due to the anticipated time required for optimization of the resist inks and printing parameters, the work was carried out at a commercial inkjet printer manufacturer. Fuji Film Dimatix was identified as a company that had the capability of doing prototype work on the length scales needed to demonstrate feasibility.

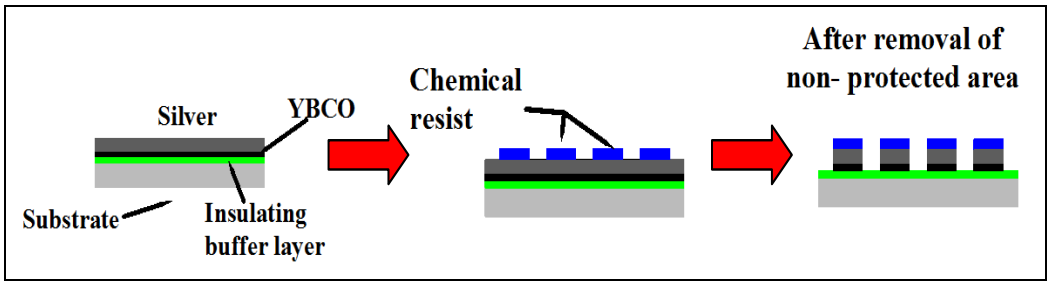

Fig. 22. Process of chemically etching silver-stabilized YBCO coated conductor to produce filamentary structures. Starting from coated conductor and moving from left to right, chemical resist is inkjet deposited onto the tape and is followed by a chemical etch to remove the silver and YBCO between the covered regions.

Two potential chemical resist materials, Microposit 1813 and a proprietary Fuji Film resist, were tested at Fuji Film Dimatix. The resist materials were printed on short length samples (10-20 cm long) of Ag coated YBCO conductor strips. After the chemical resist was cured, samples were returned for removal of the silver and YBCO layers and final characterization of the materials.

The results from this effort were not successful as each material had different issues in the process. The micrograph in Figure 23 shows the Microposit 1813 had difficulties jetting in the print head, producing very inconsistent patterns on the strip. The proprietary FujiFilm resist was able to be inkjet deposited in well-defined patterns as shown in Figure 24, but did survive the etching process as the covered areas etched at a higher rate than areas in between the covered areas. Given the mixed results from these materials, no additional effort was carried out during the Phase I project.

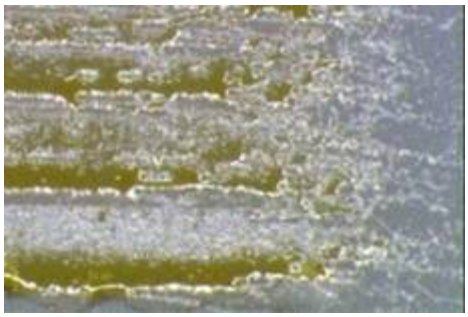

Fig. 23. Image of silver stabilized YBCO coated conductor after inkjet deposition of Microposit 1813.

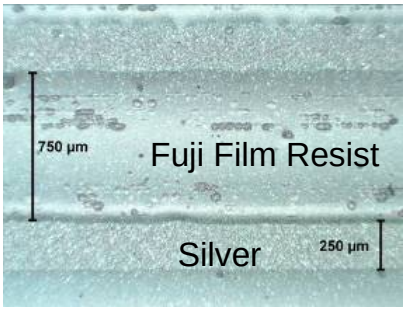

Fig. 24. Image of silver stabilized YBCO coated conductor after inkjet deposition of proprietary Fuji Film resist.

SUMMARY

Although direct inkjet printing is an attractive technique for depositing YBCO films, the results of the project shows it is not a practical method for depositing thick (>1 mm) YBCO filaments with at the widths required for low ac loss conductors. Although the YBCO filaments can be precisely printed with the targeted dimensions, the ink interaction with the substrate produces a rounded cross-sectional profile. This profile is exaggerated as the filament width narrows. The non-uniform filament thickness effects the YBCO nucleation and growth resulting in a severe reduction in the overall Jc of the patterned film. Unless the growth conditions can be modified to accommodate the filament non-uniformities, the inkjet printing technology will not be a viable process for producing YBCO films with the quality required for commercial conductors.

REFERENCES

1 M.W. Rupich, X. Li, C. Thieme, S. Sathyamurthy, S. Fleshler, D. Tucker, E. Thompson, J. Schreiber, J. Lynch, D. Buczek, K. DeMoranville, J. Inch, P. Cedrone, and J. Slack, Supercond. Sci. Technol, (in press).

2 A.P. Malozemoff, S. Fleshler, M. Rupich, C. Thieme, X. Li, W. Zhang, A. Otto, J. Maguire, D. Folts, Y. Yuan, H-P. Kraemer, W. Schmidt, M. Wohlfart and N-W. Neumueller, Superconductor Science and Technology, 21, 034005 (2008).

3 X. Li, M.W. Rupich, C.L.H. Thieme, M. Teplitsky, S. Sathyamurthy, E. Thompson, D. Buczek, J. Schreiber, K. DeMoranville, J, Lynch, J. Inch, D. Tucker, R. Savoy and S. Fleshler IEEE Transactions on Applied Superconductivity, 10, 3231(2009).

4 M.W. Rupich, U. Schoop, D.T. Verebelyi, C. Thieme, W. Zhang, X. Li, T. Kodenkandath, N. Nguyen, E. Siegal, D. Buczek, J. Lynch, M. Jowett, E. Thompson, J-S. Wang, J. Scudiere, A.P. Malozemoff , Q. Li, S. Annavarapu, S. Cui, L. Fritzemeier, B. Aldrich, C. Craven, F. Niu, A. Goyal, M. Paranthaman, IEEE Transactions on Applied Superconductivity, 13, 2458 (2003).

5 A.P. Malozemoff, S. Fleshler, M. Rupich, C. Thieme, X. Li, et al., Superconductor Science and Technology, 21, 034005 (2008)

6 S. Fleshler, M. Rupich and A.P. Malozemoff, “Scale-up of 2G HTS Wire Manufacturing at American Superconductor Corporation ,”DOE Peer Review 2007, (Crystal City, VA, August 7, 2007) http://www.energetics.com/supercon07/pdfs/AMSCScale-up.pdf

7 S. Fleshler and M. Rupich, “AMSC 2G Wire Technology,” 2009 High Temperature Superconductivity Program Peer Review, Alexandria, VA, August 4 – 5, 2009 http://www.htspeerreview.com/pdfs/presentations/day%201/joint/1-Joint-American-2G-Wire-Technology.pdf

8. M W. Rupich, D. Verebelyi, C. Thieme, U. Schoop, X. Li, T. Kodenkandath, W. Zhang, M. Teplitsky, J. Scudiere, A. Goyal and M. Paranthaman “Development of 2G YBCO-RABiTS Wires,” 2003 Annual Superconductivity Peer Review, Washington, DC, July 23-25, 2003 http://www.htspeerreview.com/2003/pdfs/presentations/e1_pres.pdf.

9. P. C. McIntyre, M. J. Cima, A. Roshko, J. Appl. Phys. 77, 5263 (1995).

10. P. C. McIntyre, M. J. Cima M.F. Ng, J. Appl. Phys. 68, 4183 (1990).

11. J.A. Smith, M. J. Cima, M, N. Sonnenberg, IEEE Trans. Appl. Super. 9, 1531 (1999).

12. M. Rupich, Q. Li, S. Annavarapu, C. Thieme, W. Zhang, V. Prunier, M. Paranthaman,

A. Goyal, D. Lee, E.D. Specht, and F. List, IEEE Trans. Appl. Superc. 11, 2927 (2001).

13. W.T. Norris, J. Phys. D3, 489 (1970).
14. E. Zeldov, J.R. Clem, M. McElfresh, and M. Darwin, Phys. Rev. B49, 9802 (1994).
15. C.E. Oberly, G.L. Rhoads, P.N. Barnes, L. Long, D.J. Scott, and W.J. Carr, Jr. Advances of Cryog. Engr. 48, 621 (2002).

16 V. Selvamanickam, Y. Xie, Y. Chen, X. Xiong, M. Martchevski, Y. Qiao, A. Rar, B. Gogia, R. Schmidt, A. Knoll, and K. Lenseth, "Progress in Scale-up of 2G HTS Wire at SuperPower," 2008 Superconductivity for Electric Systems Peer Review, Arlington, VA, July 29 – 31, 2008 http://www.htspeerreview.com/2008/pdfs/presentations/tuesday/joint/joint_2_scale_up_progress_superpower.pdf.

17 T. Mouganie and B. A. Glowacki, Journal of Materials Science, 41, 8257 (2006).

18 T. Mouganie and B.A. Glowacki, MRS Proceedings, 860, LL3.8 (2004).

19 R.C. Duckworth, M. Parans Paranthaman, M.S. Bhuiyan, F.A. List, and M.J. Gouge, IEEE Transactions on Applied Superconductivity, 17, 2,3159 (2007).

20 W.J. Carr, AC Loss and Macroscopic Theory of Superconductivity, 2nd ed.,Gordon and Beach: London, 2001.